CrossMark

REGULAR PAPER

Cuicui Zhang · Hao Wei · Chongke Bi · Zhilei Liu

Helmholtz–Hodge decomposition-based 2D and 3D ocean surface current visualization for mesoscale eddy detection

Abstract Ocean surface current (or ocean flow) visualization plays a significant role in the understanding of dynamical processes of ocean. It has been a hot research topic in both computer science and oceanography. Ocean surface current is a turbulent flow field mixing of multi-scale ocean dynamics such as large-scale ocean circulations (100 km ∼), mesoscale eddies (10–100 km), submesoscale processes (1–10 km). Mesoscale eddies, which are strong but short-life movement relative to the large-scale ocean circulations, have great importance on the transportation of ocean water masses, momentum and energy. However, their detection and recognition, which are treated as the foundation of exploring their dynamical mechanisms, is still a challenging issue. For one thing, in the mixed ocean flow field, different ocean flows depended and influence with each other making existing methods difficult to identify among them. For another, mesoscale eddies are active signals on the ocean. They may change their forms and velocities at any time. This challenges existing works to deal with their boundary ambiguity and unremitting transitions. To solve these problems, this paper proposes a novel 2D and 3D ocean surface current visualization approach based on an amended Helmholtz–Hodge decomposition (HHD), which can be widely used for mesoscale eddy detection. In our method, HHD decomposes each mixed ocean flow field to two components: curl component and divergence component. Different ocean flows can be represented by these two components independently. In addition, to improve the performance of eddy identification and to reveal the 3D structure of ocean flows simultaneously, HHD transforms the 2D ocean flow field to 3D potential surfaces. Finally, comprehensive experiments are performed on both global and local ocean flow field (Black Sea and Mediterranean Sea) calculated from satellite maps of sea level anomaly to verify our method. Experimental results demonstrate the good effectiveness of our method.

1 Introduction

Ocean surface current, also known as "ocean current or ocean flow", refers to the process of comparatively stable flowing of seawater. Nevertheless, it must be affected by several inner changes of ocean and plenty of external acting forces such as wind, the Coriolis effect. The ocean surface current is a turbulent flow field

C. Zhang · H. Wei
School of Marine Science and Technology, Tianjin University, Tianjin, China

C. Bi
School of Computer Software, Tianjin University, Tianjin, China

Z. Liu (✉)
College of Intelligence and Computing, Tianjin University, Tianjin, China
E-mail: zhileiliu@tju.edu.cn

mixing of multi-scale dynamic processes such as large-scale ocean circulations (100 km ∼), mesoscale eddies (10–100 km), submesoscale processes (1–10 km). These processes affect each other and play different roles in the ocean. Ocean mesoscale eddies, including cyclonic and anticyclonic eddies, are strong but short-life ocean signals, with typical horizontal scales of less than 100 km and timescales on the order of month. The eddy field includes coherent vortices of cyclonic and anticyclonic shapes, as well as a rich cascade of other structures such as squirts, filaments and spirals. They have significant importance on the transportation of ocean water masses, momentum and energy and then affect the physical and geological process, formation and changes of weather and climate (Nencioli et al. 2010; Zhang et al. 2014). The detection and recognition of mesoscale eddies is an very important research topic in many fields such as fishery, navigation, climate change prediction, pollution discharge. (Williams et al. 2011; Samsel et al. 2015).

Traditional mesoscale eddy detection relies much on the data acquired from observation vessels, which are usually inconsistent in both spatial and temporal domain. This limits the performance of detection algorithms. Recently, with the fast development of high-resolution ocean observation satellites, the identification of characteristics ocean flows such as mesoscale eddies has been greatly activated and promoted. The detection and tracking of mesoscale and submesoscale eddies from the satellite-observed sea surface temperature (SST), sea surface height (SSH), sea level anomaly (SLA) have become possible (Tandeo et al. 2013; Xiu et al. 2010; Zheng et al. 2011). However, the detection of eddies from the 2D ocean flow field is not an easy task. Since the 2D ocean surface current is a mixture of variant ocean flows, different ocean flows depend and influence with each other, making the 2D flow field chaotic. This high dependence and mixture of each other challenging existing methods in distinguishing between them. Moreover, existing methods are very difficult to deal with the boundary ambiguity and unremitting transitions between different dynamic processes in the 2D field. Even worse, small-scale mesoscale eddies may be hidden by larger ocean circulations in the 2D view.

The difficulties in mesoscale eddy detection are tripartite. Firstly, we need to develop an appropriate ocean flow visualization algorithm for the representation and modeling of various ocean flows, especially for characteristic ocean flows including mesoscale eddies, upwelling (divergence) and downwelling (convergence). Ocean flow modeling and visualization, which is the foundation of understanding the dynamic process of oceans flows and exploring their dynamical mechanisms, plays a significant role in the detection and recognition of mesoscale eddies (Ren et al. 2013). However, there is not yet a most suitable ocean flow visualization algorithm, which can depict different ocean flows using different interpretations. The prevailing paradigms for flow visualization include three basic forms: the hedgehog, flow lines (or trajectories), and dense vector field (Zhu and Ii 1995). The first kind of technique draws arrows of different lengths at grid points to represent the flow magnitude and direction. Although the performance of this kind of method is relatively stable, its application fields are very limited because this technique lacks the continuity in representing ocean flows in both spatial and temporal domain (Zhu and Ii 1995; Yang et al. 2018). The second kind of methods mainly refers to the particle-based techniques, such as streamlines, stream surfaces, particle traces. (Liu et al. 2003; Sun 2006; Tao et al. 2014; Ji et al. 2016; Liu and Robert Moorhead 2017; Bi et al. 2017, 2018). Although this kind of technique can show detailed local flow properties, it cannot illustrate the global view of motion without an exhaustive generation of streamlines. They can only be used for visualization of steady or slow-flow fields such as the large-scale mean flow or ocean circulation. The third kind of technique utilizes dense vector field to represent ocean flows. It is developed based on vector field topologies. This kind of method, e.g., Liu et al. (2003) visualized the detailed flow mechanism in a closed region. However, multiple different ocean flows are mixed in the 2D dense motion field making existing methods difficult to identify the features of different ocean flows.

Secondly, we need to develop an effective characteristic ocean flow extraction algorithm for the detection and identification of eddy structures (Zhu and Ii 1995). Existing mesoscale eddy detection (also known as recognition, segmentation, tracking) methods can be generally divided into two groups: physical parameter-based methods and geometric structure-based methods (Petersen et al. 2013). The first type of methods detects mesoscale eddies using the values of specified physical parameters. The most widely used method is the Okubo–Weiss method (Isernfontanet et al. 2003; Chelton et al. 2011), which utilizes Okubo–Weiss (OW) parameter W as a measurement of strain versus vorticity to identify eddies. In this kind of methods, the regions that exceed a certain predefined threshold are recognized as eddies. The second type of methods recognizes eddies using the curvature or shape of the instantaneous geometric representations of ocean flows, such as streamlines (Sadarjoen and Post 2000). This kind of methods search for reversals in velocity field (Nencioli et al. 2010) or streamlines with circular or elliptical closed geometry as eddies (Liu et al. 2015). The most well-known method of this group is the winding-angle (WA) method (Souza et al.

2011). Although existing methods can detect mesoscale eddies in the simple situation roughly, their performances are not always effective especially with complex environments. For one thing, since the setting of physical parameters relies much on the experience of expert system (or prior knowledge), it is not always available in many situations and thus the detection fails. For another, the geometric patterns of the second method are not sophisticated enough to represent complex eddy structures. In addition, little efforts have been put on the identification of other characteristic ocean flows such as the divergent upwelling and convergent downwelling ocean flows.

Thirdly, it would be better transform the 2D velocity field to higher-dimensional space such as 3D space in order for more accurate segmentation of characteristic ocean flows and the reconstruction of whole 3D structure of mesoscale eddies. Existing works identify mesoscale eddies from the original ocean flow field directly. Since multi-scaled processes (large-scale, mesoscale, submesoscale) are mixed and dependent with each other, the segmentation of characteristic ocean flows (e.g., mesoscale eddies) from the complex ocean flow is very challenging. Thus, the performance of existing methods is not satisfactory and they cannot be widely applied to generic ocean flows. What's more, existing works detect characteristic ocean flows from the 2D vector field other than in higher-dimensional spaces (e.g., the 3D space). They cannot know about the 3D structures of them. That means, the depth of characteristic ocean flows is unknown for existing works and they have no idea on how deep do characteristic ocean flows go and effect. Actually, the reconstruction of 3D shape of mesoscale eddies is quite important in analyzing their mass and energy transport in the global ocean flow field (Zhang et al. 2014, 2017). However, Oceanographers are confused by such questions as how deep are ocean eddies? Do they look more like thin disks or tall columns? Do eddies with large surface extents tend to be deeper or not? (Petersen et al. 2013).

Due to the three main challenging issues, the performance of existing methods is still far from satisfactory especially for complex eddy identification. Moreover, few works have been developed to investigate the 3D structure of eddies and none of them have focused on the detection and identification of other characteristic ocean flows (upwelling and downwelling). In addition, the depth information of the eddies (including cyclonic and anticyclonic eddies) as well as their distributions in the global ocean flow field has not yet been studied in the literature. To solve these problems, this paper proposes a novel 2D and 3D ocean flows visualization method based on an amended Helmholtz–Hodge decomposition, which can be used for the identification of cyclonic and anticyclonic mesoscale eddies. Our method solves the above-mentioned issues by introducing HHD, which partitions an arbitrary ocean field to two components: a curl component and a divergence component. Different characteristic ocean flows can be modeled by these two components independently so that the dependence and influence of them can be released. Moreover, HHD transforms the 2D vector field to 3D potential surfaces, thereby we can reveal the 3D structure of mesoscale eddies and know about how deep do eddies go and effect. Finally, by applying our method to satellite-observed ocean velocity data obtained from MSLA, we investigate the 3D properties of characteristic ocean flows such as their distributions and depth information in both regional and global ocean.

1.1 Overview of our approach

To take advantage of 2D and 3D structure investigation of ocean flows, in this paper, we develop a novel ocean flow decomposition method based on Helmholtz–Hodge decomposition for the 2D and 3D visualization of characteristic ocean flows as well as for mesoscale eddy detection. The pipeline of our method is illustrated in Fig. 1. HHD first transforms the original 2D vector field (obtained from MSLA) to two 3D potential surfaces: a vectorial potential surface and a scalar potential surface. Next, two components of HHD: curl component and divergence component are calculated from these two potential surfaces, respectively. Then, different characteristic ocean flows can be represented by using these two components independently. Finally, we extract the featured vortices of eddies from the curl component accurately. We can see that the 3D potential surfaces of HHD reveal the 3D structure of characteristic ocean flows including their depth information and distributions clearly.

1.2 Contributions

The primary contributions of this paper are:

- A HHD-based ocean flow decomposition method is developed for 2D and 3D modeling and visualization of complex ocean flow fields so that different characteristic ocean flows (eddies and divergence ocean flows) can be represented by different components independently.
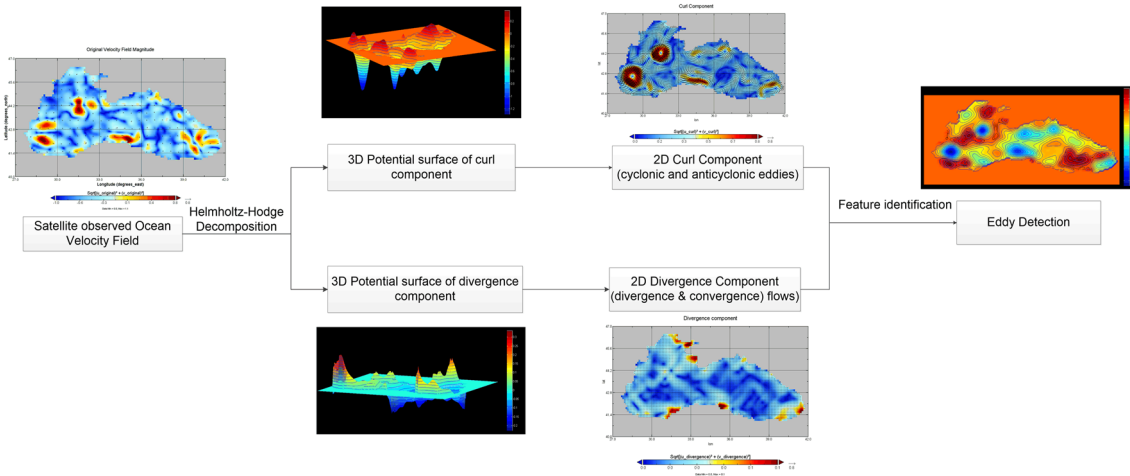
Fig. 1 The pipeline of our method: HHD first transforms the original 2D vector field to two 3D potential surfaces: a vectorial potential surface and a scalar potential surface. Two components of HHD: curl component and divergence component are then calculated from these two potential surfaces, respectively. After that, different characteristic ocean flows can be represented by these two components independently. Finally, we extract the featured vortices of eddies from the curl component accurately

- The 3D potential surfaces obtained from HHD reveal the depth and distribution of eddy structures, which answers the question of how deep mesoscale eddies go and effect. To our knowledge, this is the first ocean flow visualization algorithm, which explores the 3D structure of characteristic ocean flows.
- An empirical study on MSLA-based ocean flow fields shows the effectiveness of our method in both regional and global ocean.

The rest of this paper is organized as follows: Sect. 2 describes ocean flow representation as well as the properties of four kinds of characteristic ocean flows: cyclonic and anticyclonic eddy, upwelling and downwelling. Section 3 introduces the principle of HHD and explains how to use HHD for the 2D and 3D visualization of characteristic ocean flows and eddy extraction. Experimental results are shown in Sect. 4, which prove the good performance of our method. Finally, Sect. 5 concludes this paper with future plans.

2 Characteristic ocean flow representation

The ocean flow conducted in this paper refers to the gridded oceanic velocity field, which is calculated from satellite maps of sea level anomaly (MSLA). The advent of sea level anomaly observations from satellite radar altimeters provided researchers with data that are more intimately related to ocean eddy activity than the previous data. The ocean velocity field is in the form of (u, v) at each grid point, where u represents the ocean flow toward the x-axis and v represents the ocean flow toward the y-axis. The magnitude is $sqrt(u^2 + v^2)$. Apart from the gridded vector field, the ocean flow field can also be represented by some numerical calculus. Most well-knowns are the curl–divergence calculation of the vector field. The curl component demonstrates the rotation of flow in the 3D space, and the divergence component (including the divergence and convergence) demonstrates the upwelling (divergence) and downwelling (convergence) ocean flow.

In this section, each characteristic ocean flow (cyclonic and anticyclonic eddy, upwelling and downwelling) is described numerically and visually. They play significant roles in understanding ocean dynamics.

2.1 Cyclonic and anticyclonic eddies

The mesoscale and submesoscale eddies refer to the rotational vector field (curl) of ocean flow. An example of eddy structure is shown in Fig. 2a. In the literature, eddies can be further classified to cyclonic and anticyclonic eddies according to their rotational directions. If the ocean moves in a counterclockwise direction in the northern hemisphere, then the rotation is called a cyclonic eddy; otherwise, it is called anticyclonic eddy. This definition is opposite in the southern hemisphere. The cyclonic eddies cause a decrease in sea level anomaly and elevations in subsurface density surfaces. That means, the center of the
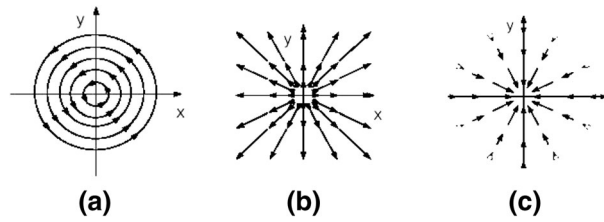
Fig. 2 Three kinds of featured vector fields: **a** rotation, also known as eddies (or curl); **b** divergence, in which vectors directed from a "source" to around; **c** convergence, in which vectors pointed to a central "sink"
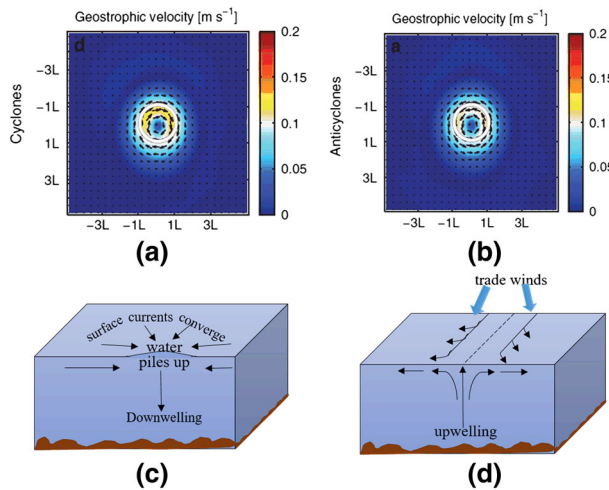

Fig. 3 Four kinds of characteristic ocean flows: **a** cyclonic eddy; **b** anticyclonic eddy; **c** downwelling (convergence); **d** upwelling (divergence)

eddy is likely cooler and lower in height (by a few tens of centimeters) than the outerlying waters. In contrast, the anticyclonic eddies cause an increase in sea level anomaly and depressions in subsurface density surfaces. That is, its center is warmer and higher (by a few tens of centimeters) than outerlying waters. In the oceanography, the cyclonic eddy is also called a cold-core eddy while the anticyclonic eddy is also called a warm-core eddy. An example of cyclonic and anticyclonic eddy in the southern hemisphere is shown in Fig. 3a, b, respectively.

2.2 Upwelling and downwelling ocean flows

Associated with eddies, there are other two kinds of characteristic ocean flows named as upwelling and downwelling flows. Winds from the overlying atmospheric circulation patterns can produce ocean surface currents that sometimes cause convergence (coming together) or divergence (moving apart) of upper ocean waters over ocean surface several kilometers in scale. Under the divergent conditions, nutrient-rich and cool waters can up well (move vertically toward the surface) from deeper waters to act as a seed for the formation of a cold-core eddy. Likewise, nutrient-poor but warmer waters may converge, be down-welled, and a warm-core eddy can form. These two kinds of vertical ocean flows which associate with the formation of eddies are known as the upwelling and downwelling ocean flows, respectively. An example of downwelling and upwelling ocean flow is illustrated in Fig. 3c, d, respectively. They can be represented by the divergence and convergence of vector field shown in Fig. 2b, c, respectively.

As we can see that the cyclonic and anticyclonic eddies are represented by rotational vector field while upwelling and downwelling ocean flows are represented by the divergence and convergence vector field. Next, we will present how to use the two components (curl and divergence) of Helmholtz–Hodge decomposition to interpret these characteristic ocean flows.

3 Ocean flow modeling and visualization using Helmholtz–Hodge decomposition

The ocean flow field is a complex vector field mixing of large-scale ocean circulations, mesoscale and submesoscale dynamic processes. As the eddy and divergent ocean flows have variant interpretations, they cannot be represented by a uniform interpretation. Thus, an invariant ocean flow representation for each kind of characteristic ocean flow needs to be developed. In this paper, we propose a vector field partition algorithm using Helmholtz–Hodge decomposition to depict eddy and divergent ocean flows by the curl–divergence regularizers of HHD.

This section presents how to use HHD for the 2D and 3D visualization of characteristic ocean flows. First, we describe the principle of HHD theoretically. Then, HHD is used to represent the 2D and 3D structure of eddies and divergent ocean flows. Finally, the identification of featured ocean flows is described.

3.1 Principle of Helmholtz–Hodge decomposition

HHD is a well-known vector field decomposition algorithm in computational fluid dynamics (CFD), which has been widely used in many research fields such as fluid dynamics modeling, flow understanding, motion analysis, camera motion segmentation, feature extraction from vector field. (Wiebel 2004; Petronetto et al. 2010; Bhatia et al. 2013; Zhang et al. 2013, 2018; Liang et al. 2014, 2015; Zhang and Liu 2017).

HHD was initially proposed by Helmholtz and Hodge, inspired that "If we know the divergence and the curl of a vector field then we know everything there is to know about the vector field." That means we can use the divergence-curl regularizers of HHD to represent an arbitrary vector field. Theoretically, HHD can decompose each ocean flow field ξ to two components: a divergence component (also named as curl-free) ∇E and a curl component (also named as divergence-free) $\nabla \times W$. This is mathematically explanation of the well-known Helmholtz–Hodge decomposition algorithm, which is defined in Eq. (1) and illustrated in Fig. 4.

$$\xi = \nabla E + \nabla \times W. \tag{1}$$
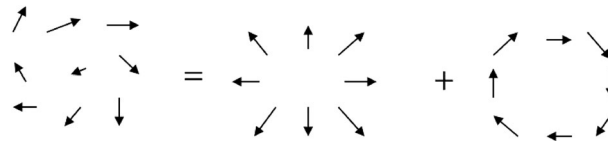
Here, E and W refer to the two 3D potential surfaces defined as: (1) *Scalar potential surface* ∇E, the gradient of which is the divergence component; (2) *Vector potential surface* $\nabla \times \vec{W}$, the curl operation of which represents the curl component (Bhatia et al. 2013). The relationship between 'curl' operator and gradient operator is as follows:
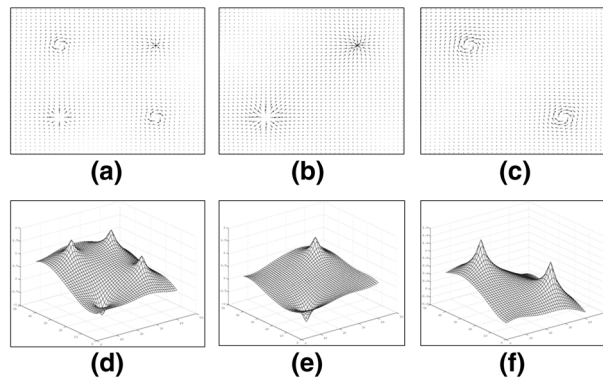

Fig. 4 HHD-based vector field decomposition: **a** the original 2D vector field and its 3D potential surface (**b**); **c** the 2D divergence component obtained from 3D potential surface E (**d**); **e** the 2D curl component obtained from 3D potential surface W (**f**)

$$\nabla \times \vec{W} = (\nabla W)^{\perp}. \tag{2}$$

The characteristic ocean flows and the background large-scale ocean mean flow can be represented by these two components independently as follows:

- The convergent and divergent ocean flow, which are irrotational, can be interpreted by the divergence component of HHD;
- The cyclonic and anticyclonic eddies, which are incompressible, can be interpreted by the curl component of HHD.
- The background large-scale mean ocean flow, which is irrotational and incompressible, can be interpreted by both curl component and divergence component equally.

From Fig. 4, we can see that there are four characteristics ocean flows in the original ocean flow field (a): one convergent ocean flow, one divergent ocean flow, and two rotational eddies. After HHD, the convergent and divergent ocean flow only exist in the divergence component (b) and the eddies only exist in the curl component (c). That means, we can use the two components of HHD to interpret different kinds of characteristic ocean flows independently.

For the implementation of HHD, variant methods have been developed in the literature (Bhatia et al. 2013). Polthier and Preu (2003) proposed a technique for implementation on 2D discrete vector fields. Tong et al. (2003) improved it and expanded it to discrete vector fields on 3D meshes. To make HHD be able to identify the background mean flow as one segment, we add two assumptions to the previously defined HHD and introduce an amended HHD for characteristic ocean flow modeling in this paper. The two assumptions are: (1) the original ocean flow field should be piece-wise smooth; (2) the background large-scale ocean flow field should also be piece-wise smooth. The implementation of HHD is as follows: since ∇E and $\nabla \times \vec{W}$ are the projection of the original ocean flow field $\vec{\xi}$ to the space of the divergence field and the curl field, the distance between $\vec{\xi}$ and two projected components should be minimized. Then, we utilize energy minimization to calculate the two components of HHD as follows:

$$\min(D(E)) = \min\left(\int_{\Omega} \| \nabla E - \vec{\xi} \|^2 \, d\Omega\right),$$

$$\min(G(\vec{W})) = \min\left(\int_{\Omega} \| \nabla \times \vec{W} - \vec{\xi} \|^2 \, d\Omega\right). \tag{3}$$

where Ω depicts the ocean flow grid domain. According to the definition of HHD, the curl component $(\nabla \times \vec{W})$ does not show in the divergence component (∇E). And vice versa. Then, we can have the following criteria:

$$\int_{\Omega} \nabla \times (\nabla E) d\Omega = \int_{\Omega} \nabla \times (\vec{\xi} - \nabla \times \vec{W}) d\Omega = 0,$$

$$\int_{\Omega} \nabla \cdot (\nabla \times \vec{W}) d\Omega = \int_{\Omega} \nabla \cdot (\vec{\xi} - \nabla E) d\Omega = 0. \tag{4}$$

Equation (4) can be rewritten in the discrete domain as:

$$\sum_{i \in \Omega} \nabla \cdot (\nabla E_i) = \sum_{i \in \Omega} \nabla \vec{\xi}_i.$$

$$\sum_{i \in \Omega} \nabla \times (\nabla \times \vec{W}_i) = \sum_{i \in \Omega} \nabla \times \vec{\xi}_i, \tag{5}$$

Since they are linear functions, we can abbreviate them as follows:

$$S_1 E = B, \qquad S_2 W = C. \tag{6}$$

where S_1 and S_2 are $N \times N$ sparse element matrices (N is the total number of the nodes on the grid domain Ω), E and W are $N \times 1$ vectors to be calculated, B and C represent the right side of Eq. (5).

The potential surfaces E and W can be calculated by solving Eq. (6). Then, $\nabla \times \vec{W}$ is obtained by Eq. (2) subsequently.

3.2 2D and 3D modeling and visualization of ocean flows using HHD

As aforementioned, HHD states that any vector field can be uniquely decomposed into a sum of a divergence and a curl component. It provides us the opportunity to recognize different ocean flows from different components independently. Moreover, HHD has the capability to reveal the 3D structure of ocean flows by using its potential surfaces, which can be recognized as the integral of vector fields in a given region.

Actually, the study of the 3D structure of ocean flow is very important. Although the mesoscale eddies have been ubiquitously observed since 1960s, the estimation of their 3D structures is still fragmentary because of the lack of systematic full water-depth observations (Zhang et al. 2016). In this paper, HHD estimates the 3D structure of eddies by using its potential surface, which answers how deep do mesoscale eddies go and effect. The merits of 3D structure reconstruction can be summarized as:

- The 3D structure reveals the shape of variant ocean flows more clearly. We can easily distinguish between cyclonic and anticyclonic eddies in the 3D space.
- Through estimating the depth of the vector field, it answers the question, how deep do mesoscale eddies go and effect?
- It discovers the hidden eddies and divergence flows according to the 3D structure of them under complex environments.

Here, we use an example to illustrate this process. We use the ocean velocity field of a study area of Black Sea (40.5°N–47°N, 27°E–42°E). The temporal and spatial resolution of this data is daily and $1°/8°$ (12.5 km). The original ocean flow data with the 2D and 3D visualization of eddies are shown in Fig. 5. From Fig. 5, we can see that by mapping the 2D vector field onto 3D potential surfaces, HHD estimates the depth of the vector field and reveals the 3D structure of mesoscale eddies clearly. Moreover, we can identify between the cyclonic and anticyclonic eddies much easier according to their 3D substructures: The blue surface, which is below zero plan, shows the cyclonic eddies; the red surface, which is above the zero plan, shows the anticyclonic eddies in the northern hemisphere.

3.3 Extraction of ocean flow features

Another purpose of using HHD for the visualization of the ocean flow is to recognize and segment featured ocean motions, such as the vortices of eddies (in the curl component). Next, we will explain the numerical identification and segmentation of these features.

The properties of the curl component for the identification of these features can be summarized as follows:
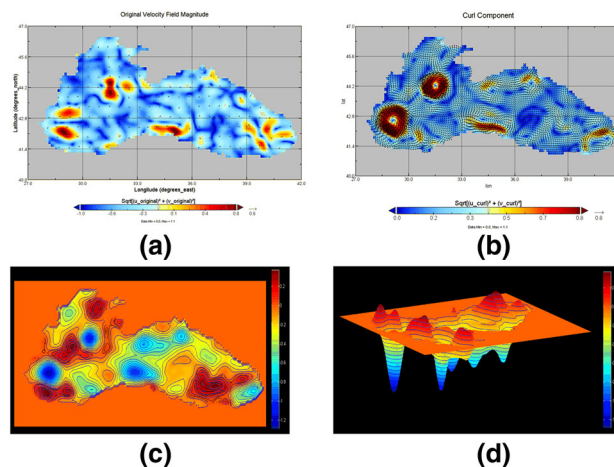

Fig. 5 The original ocean flow field and the 2D and 3D visualization of the mesoscale eddies in the Black Sea: **a** the original ocean flow field; **b** the calculated curl component of from HHD; **c** the 2D visualization of the curl component; **d** the 3D visualization of the curl component
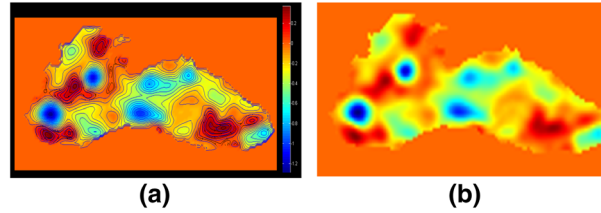
Fig. 6 The detection of mesoscale eddies in the curl component in Black Sea: **a** the 2D visualization of the curl component; **b** the detection of vortices from the curl component

- *Cyclonic eddy* In the 2D vector field, the cyclonic eddy refers to the vector field which rotates around the center vortex in the anticyclonic way in the northern hemisphere. On the 3D potential surfaces, the cyclonic eddy is represented by the surface below the zero plan (depth < 0).
- *Anticyclonic eddy* The anticyclonic eddies differ with cyclonic eddies in the rotating direction. It rotates around the center vortex in the cyclonic way in the northern hemisphere. On the 3D potential surfaces, the anticyclonic eddy is represented by the surface above the zero plan (depth > 0).

The detection of vortices in the Black Sea is shown in Fig. 6.

4 Experiments

4.1 Data

Experiments are performed on the satellite-observed ocean flow data. The geostrophic ocean flow field formed in (u, v) is calculated from the satellite maps of sea level anomaly (MSLA). The MSLA and its calculated ocean velocity data, ranging from 1993 to the ongoing, are obtained from delayed-time reference series provided by Archiving, Validation and Interpretation of Satellite Data in Oceanography (AVISO) center. This dataset includes both local ocean (Mediterranean Sea, Black Sea, European Seas, Arctic Ocean areas) data and worldwide global ocean data. In this paper, we performed experiments on both regional and global ocean data for comprehensive evaluation. The study areas include: the Black Sea (40.5°N–47°N, 27°E–42°E), the Mediterranean Sea (30.0625°N–45.9375°N, 354.0625°E–396.937°E) and the global ocean (90°S–90°N, 180°E–180°W). Thanking the advanced geographical location and geography factors, many mesoscale eddies appear in the Black Sea and Mediterranean Sea. They have become two most representative regions for mesoscale eddy observation in the satellite maps (Faghmous et al. 2015; Mkhinini et al. 2015). The spatial resolution of regional ocean data (Mediterranean Sea and Black Sea) is 1°/8° (12.5 km), which is twice higher than that for the global ocean data (1°/4°); the temporal resolution is seven days (delayed time product) (Faghmous et al. 2015; Mkhinini et al. 2015). The data we used are obtained during September 2017.

The fields of the geostrophic velocity were calculated using the sea level anomaly maps from the geostrophic balance equations by:

$$u = -\frac{g}{f}\frac{\partial h}{\partial y},$$
$$v = \frac{g}{f}\frac{\partial h}{\partial x},$$

where u and v are the zonal (horizontal) and meridional (vertical) components of the geostrophic velocity, g is the acceleration of gravity, f depicts the Coriolis parameter, and h is the sea level anomaly.

4.2 Experimental results

To use this visualization system, we first need to prepare the ocean flow data formatted in (u, v) as mentioned above (this data can be acquired from AVISO data center or be obtained from in situ hydrological observation systems), then we can input the data to this visualization system and calculate the curl and divergence component using the Helmholtz–Hodge decomposition method explained in Sect. 3.1. Finally, the 2D and 3D visualization of characteristic ocean flows (including the mesoscale eddies, the upwelling and

downwelling ocean flows) can be visualized using the curl and divergence component as explained in Sects. 3.2 and 3.3. The experimental results in variant regions (including the Black Sea, the Mediterranean Sea, and the global ocean flow field) are shown and explained as follows.

Black Sea Mesoscale eddies are the essential parts of dynamic processes in the Black Sea basin 40.5°N–47°N, 27°E–42°E. In this paper, we use the proposed method to study the characteristics and structure of ocean flows and visualize them in both 2D and 3D spaces.

The experimental result in the Black Sea is shown in Fig. 7. Figure 7a shows the original ocean velocity data, whose resolution is $1°/8° \times 1°/8°$. Colors are used to depict the magnitude of ocean flow. From Fig. 7a, we can see that it is very difficult to identify eddies from the mixed velocity field directly. Figure 7b, c demonstrates the curl component and divergence component, respectively. We can find that the eddies and the divergence ocean flows can be represented by these two components clearly: The rotating structure in the curl component depicts the mesoscale eddies; the divergence and convergence ocean flows are separated from the eddies, which only exist in the divergence component. That is, HHD helps us identify different kinds of characteristic ocean flows from different components independently. Figure 7d, e shows the corresponding 3D potential surface of the curl component and the divergence component. We can see that the 3D potential surfaces reveal the 3D structure of ocean flows vividly. It can also help us identify different mesoscale eddies (cyclonic and anticyclonic eddies) distinctly: the rotating eddies below the planar surface (in blue color) represents the cyclonic eddies while the rotating structure above the planar surface (in red color) represents the anticyclonic eddies. In addition, the 3D potential surface estimates the depth information of eddies and answers how deep do mesoscale eddies go and effect. Finally, the detected vortices are shown in Fig. 7f, which helps us in understanding the dynamic process of mesoscale eddies. The experimental result proves the effectiveness of our method in visualizing the 2D and 3D structure of characteristic ocean flows.

Mediterranean Sea The Mediterranean Sea, which is located at 30.0625°N–45.9375°N, 354.0625°E–396.937°E, is dominated by complex ocean circulation dynamical systems. In many semiclosed and closed seas, the ocean circulation is dominated by gyres (large system of circulating ocean currents) and coastal eddies, and the kinetic energy of the instantaneous eddy field is much larger than that of the long-term average circulation (mean ocean flow). This shows the just case of Mediterranean Sea, which exhibits a very complex circulation system (Mkhinini et al. 2015). Thereby, the study of the characteristic ocean flows in Mediterranean Sea is very important in understanding its ocean dynamics. The experimental result is shown in Fig. 8, where Fig. 8a shows the original ocean velocity field of resolution $1°/8° \times 1°/8°$. Similar to the last example, the 2D visualization and the 3D visualization of the curl and divergence component are shown in Fig. 8b–e, respectively. We can see that it is also very difficult to identify the eddy and divergence
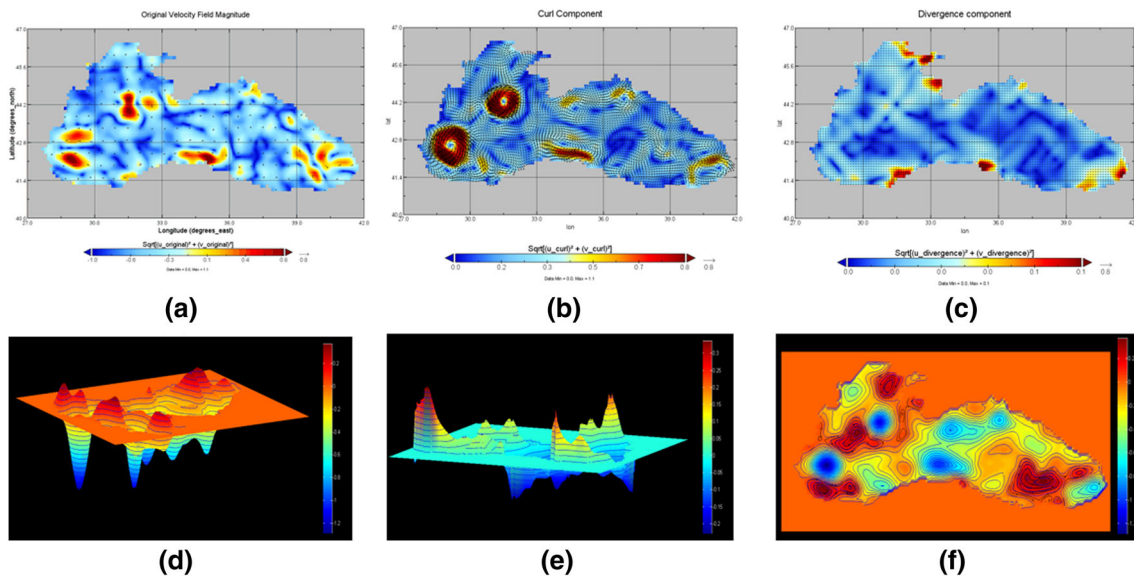

Fig. 7 Experimental results on the Black Sea: **a** the original ocean flow field; **b** the curl component of HHD; **c** the divergence component of HHD; **d** the 3D potential surface of curl component; **e** the 3D potential surface of divergence component; **f** the 2D visualization of the curl component
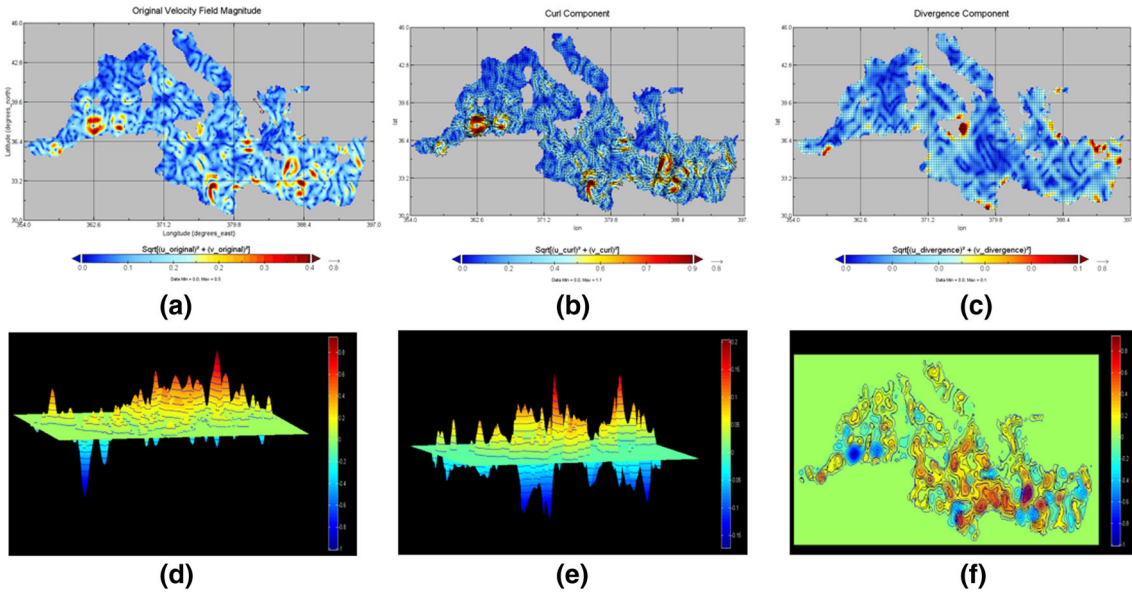
Fig. 8 Experimental results on the Mediterranean Sea: **a** the original ocean flow field; **b** the curl component of HHD; **c** the divergence component of HHD; **d** the 3D potential surface of curl component; **e** the 3D potential surface of divergence component; **f** the 2D visualization of the curl component

Fig. 9 Experimental results on the global ocean field: **a** the original ocean flow field; **b** the curl component of HHD; **c** the divergence component of HHD; **d** the 3D potential surface of curl component; **e** the 3D potential surface of divergence component; **f** the 2D visualization of the curl component
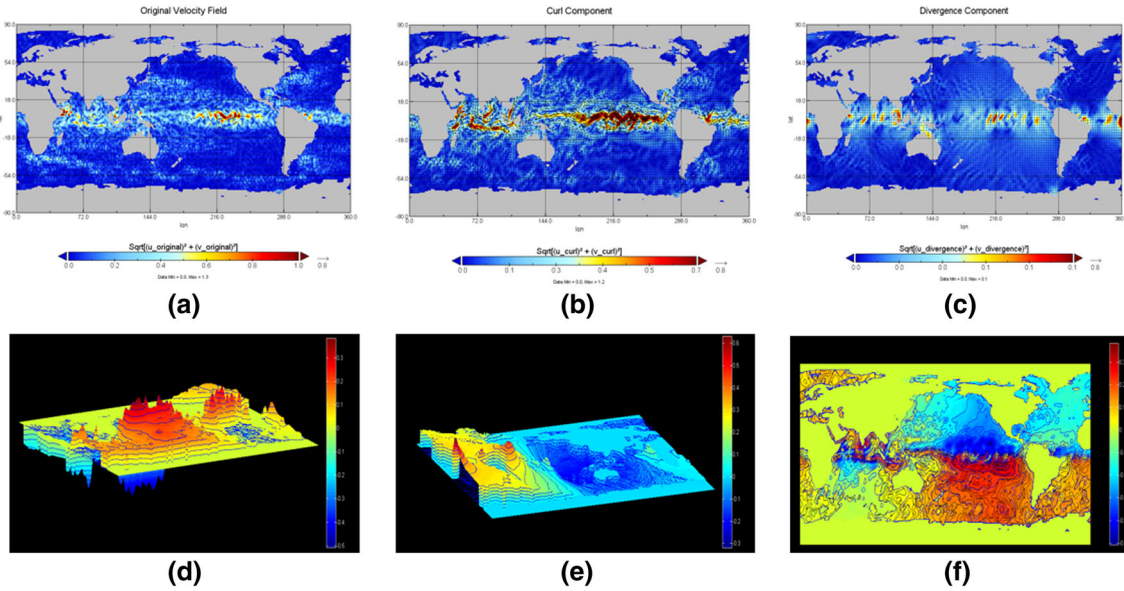
structures from the original ocean flow field in Fig. 8a. But it becomes much easier in Fig. 8b–e. Compared to the experimental results in the Black Sea, the cyclonic and anticyclonic eddies are much smaller than that in the Black Sea. Moreover, most parts of eddies locate in the eastern region of the Mediterranean Sea, which is consistent with the previous research results in Mkhinini et al. (2015). It says that the excess of evaporation in the Mediterranean Sea is mainly compensated by the fresh Atlantic Water entering through the Strait of Gibraltar. Part of the Atlantic Water, which crosses the Sicilian channel, drives the surface circulation in the Eastern Mediterranean Sea, where small eddies may generate.

Global Ocean The third experiment is performed on the global ocean (ranging from 90°S–90°N, 180°E-180°W) to demonstrate the good performance of our method in detecting characteristic ocean flows in the global ocean. The resolution of the global ocean field is half of that the regional ocean, which is $1°/4° \times 1°/4°$. The experimental result is shown in Fig. 9. Similar to the last two examples, the original flow data are shown in Fig. 9a, while Fig. 9b–e illustrates the 2D and 3D visualization of the curl and divergence component, respectively. From Fig. 9a, we can see that the original ocean flow field is too turbulent to find any eddy or divergence structures. Even worse, the regions with salient motions become unclear compared with regional oceans. We cannot find any meaningful information from this original global ocean field. In contrast to Fig. 9a, the curl and the divergence components shown in Fig. 9b, c are very useful in identifying eddy and divergence ocean flows. Moreover, the 3D visualization in Fig. 9d, e reveals the 3D structure of these featured flows, where we can estimate the depth and the distribution of eddies very clearly. This experiment verifies the effectiveness of our method in dealing with global ocean flow field.

5 Conclusion

This paper proposed a novel 2D and 3D ocean surface current visualization method using Helmholtz–Hodge decomposition (HHD), which can be used for the identification of characteristic ocean flows (cyclonic and anticyclonic mesoscale eddies, upwelling and downwelling ocean flows). Through decomposing the original ocean flow field to a curl and a divergence component, HHD allocated the eddy and the divergence ocean flows into these two components, respectively. In this way, we can detect different characteristic ocean flows from different components independently. Moreover, HHD transforms the 2D vector field to the 3D potential surfaces, which reveal the 3D structure of characteristic ocean flows in the 3D space. The 3D structure of ocean flows investigates how deep do mesoscale eddies go and effect.

Comprehensive evaluation of our method is performed on the satellite-observed ocean velocity data on both regional (Black Sea and Mediterranean Sea) and global ocean. Experimental results demonstrate that our method can visualize and identify characteristic ocean flows from even complex ocean flows accurately. The 3D structure of potential surfaces estimates the depth information and distribution of characteristic ocean flows very clearly. Actually, our method only detects characteristic ocean flows in the spatial domain without discussing their temporal characteristics. In the future, we are planning to develop spatiotemporal models to analyze the dynamic processes of ocean flows, e.g., the fusion and collision of mesoscale eddies, their appear and disappear disciplines and so on.

References

Bhatia H, Norgard G, Pascucci V, Bremer PT (2013) The Helmholtz–Hodge decomposition—a survey. IEEE Trans Vis Comput Graph 19(8):1386

Bi C, Yuan Y, Zhang J, Shi Y, Xiang Y, Wang Y, Zhang R (2018) Dynamic mode decomposition based video shot detection. IEEE Access 6:21397–21407

Bi C, Yuan Y, Zhang R, Xiang Y, Wang Y, Zhang J (2017) A dynamic mode decomposition based edge detection method for art images. IEEE Photon J 6(6):1–13

Chelton D, Schlax M, Samelson R, Early J (2011) Global satellite altimeter observations of nonlinear mesoscale eddies. Prog Oceanogr 91:167–216

Faghmous JH, Frenger I, Yao Y, Warmka R, Lindell A, Kumar V (2015) A daily global mesoscale ocean eddy dataset from satellite altimetry. Sci Data 2:150028

Isernfontanet J, Garcaladona E, Font J (2003) Identification of marine eddies from altimetric maps. J Atmos Ocean Technol 20(5):772–778

Ji P, Tian F, Liu S, Chen G (2016) 3D streamline visualization for irregular flow field data. J Comput Theor Nanosci 13(11):8909–8916

Liang X, Zhang C, Matsuyama T (2014) Inlier estimation for moving camera motion segmentation. In: Proceedings of Asian conference on computer vision (ACCV). Springer, pp 352–367

Liang X, Zhang C, Matsuyama T (2015) A general inlier estimation for moving camera motion segmentation. IPSJ Trans Comput Vis Appl 7:163–174

Liu Z, Du Y, Xu K (2015) An improved scheme of identifying loops using Lagrangian drifters. In: IEEE international conference on spatial data mining and geographical knowledge services, pp 125–128

Liu Z, James R, Scan M, Ziegeler B (2003) Ocean flow visualization in virtual environment. Technical Report, pp 1–49

Liu Z, Moorhead R II (2016) High-performance flow visualization for effective data analysis. J Flow Vis Image Process 23(1–2):41–57

Mkhinini N, Coimbra ALS, Stegner A, Arsouze T, TaupierLetage I, Branger K (2015) Longlived mesoscale eddies in the eastern Mediterranean Sea: analysis of 20 years of AVISO geostrophic velocities. J Geophys Res Oceans 119(12):8603–8626

Nencioli F, Dong C, Dickey T, Washburn L, Mcwilliams JC (2010) A vector geometry–based eddy detection algorithm and its application to a high-resolution numerical model product and high-frequency radar surface velocities in the southern california bight. J Atmos Ocean Technol 27(3):564

Petersen MR, Williams SJ, Maltrud ME, Hecht MW, Hamann B (2013) A threedimensional eddy census of a highresolution global ocean simulation. J Geophys Res Oceans 118(4):1759–1774

Petronetto F, Paiva A, Lage M, Tavares G, Lopes H, Lewiner T (2010) Meshless Helmholtz–Hodge decomposition. IEEE Trans Vis Comput Graph 16(2):338–349

Polthier K, Preu E (2003) Identifying vector fields singularities using a discrete Hodge decomposition. In: Hege HC, Polthier K (eds) Visualization and mathematics III, Mathematics and Visualization. Springer, Berlin, pp 123–134

Ren B, Li CF, Lin MC, Kim T, Hu SM (2013) Flow field modulation. IEEE Trans Vis Comput Graph 19(10):1708–19

Sadarjoen IA, Post FH (2000) Detection, quantification, and tracking of vortices using streamline geometry. Comput Graph 24(3):333–341

Samsel F, Petersen M, Abram G, Turton TL, Rogers D, Ahrens J (2015) Visualization of ocean currents and eddies in a high-resolution global ocean-climate model. In: Proceedings of the international conference on high performance computing, networking, storage and analysis, vol 2, issue 3, pp 1–4

Souza JMAC, Montgut CDB, Traon PYL (2011) Comparison between three implementations of automatic identification algorithms for the quantification and characterization of mesoscale eddies in the South Atlantic Ocean. Ocean Sci 7(3):317–334

Sun Y (2006) Visualizing oceanic and atmospheric flows with streamline splatting. Proc SPIE Int Soc Opt Eng 6060:606002–606012

Tandeo P, Chapron B, Ba S, Autret E, Fablet R (2013) Segmentation of mesoscale ocean surface dynamics using satellite SST and SSH observations. IEEE Trans Geosci Remote Sens 52(7):4227–4235

Tao J, Wang C, Shene CK, Kim SH (2014) A deformation framework for focus + context flow visualization. IEEE Trans Vis Comput Graph 20(1):42–55

Tong Y, Lombeyda S, Hirani A, Desbrum M (2003) Discrete multiscale vector field decomposition. In: ACM SIGRAPH, pp 27–31

Wiebel A (2004) Feature detection in vector fields using the Helmholtz–Hodge decomposition. Diploma Thesis, University of Kaiserslautern, pp 1–61

Williams S, Petersen M, Bremer PT, Hecht M, Pascucci V, Ahrens J, Hlawitschka M, Hamann B (2011) Adaptive extraction and quantification of geophysical vortices. IEEE Trans Vis Comput Graph 17(12):2088–2095

Xiu P, Chai F, Shi L, Xue H, Chao Y (2010) A census of eddy activities in the South China Sea during 1993–2007. J Geophys Res Atmos 115(C3):132–148

Yang L, Wang B, Zhang R, Zhou H, Wang R (2018) Analysis on location accuracy for the binocular stereo vision system. IEEE Photon J 10(1):1–16

Zhang C, Liang X, Matsuyama T (2013) Mixed-motion segmentation using Helmholtz decomposition. IPSJ Trans Comput Vis Appl 5:55–59

Zhang C, Liu Z-L (2017) Prior-free dependent motion segmentation using Helmholtz–Hodge decomposition based object-motion oriented map. J Comput Sci Technol 32(3):520–535

Zhang C, Wei H, Bi C, Liu Z (2018) Helmholtz–Hodge decomposition based 2D and 3D ocean flow visualization for mesoscale eddy detection. J Vis (ChinaVis 2018) 1–8

Zhang Z, Tian J, Bo Q, Wei Z, Ping C, Wu D, Wan X (2016) Observed 3D structure, generation, and dissipation of oceanic mesoscale eddies in the South China Sea. Sci Rep 6:24349

Zhang Z, Wang W, Qiu B (2014) Oceanic mass transport by mesoscale eddies. Science 345(6194):322–324

Zhang Z, Zhang Y, Wang W (2017) Three-compartment structure of subsurface-intensified mesoscale eddies in the ocean. J Geophys Res Oceans 122(3):1653–1664

Zheng Q, Tai CK, Hu J, Lin H, Zhang RH, Su FC, Yang X (2011) Satellite altimeter observations of nonlinear Rossby eddy–Kuroshio interaction at the Luzon Strait. J Oceanogr 67(4):365

Zhu Z, Ii RJM (1995) Extracting and visualizing ocean eddies in time-varying flow fields. In: Proceedings of the 7th international conference on flow visualization, pp 206–211